

# Palmprint Identification based on texture features using GLCM through Dynamic ROI

K.J Archana<sup>1</sup>

<sup>1</sup>CSE Department, Swami Vivekananda Institute of Technology SVIT, Secunderbaad-03,

V.Sangeetha<sup>2</sup>

<sup>2</sup>CSE Department Swami Vivekananda Institute of Technology SVIT, Secunderbaad-03.

Y. L. Malathi Latha<sup>3</sup>

<sup>3</sup>CSE Department, Swami Vivekananda Institute of Technology SVIT, Secunderbaad-03,

**Abstract:** *In this paper, a novel palmprint identification algorithm is proposed based on GLCM through dynamic ROI. Region of interest (ROI) extraction is an important task for palmprint identification. Earlier reported works used fixed size ROI for the recognition of palmprints. When the fixed size ROI is used the palm area taken up for recognition is less compared to dynamic ROI extraction. The proposed algorithm focuses on extraction of maximum possible ROI. Texture features are extracted using GLCM from dynamic ROI image. The experimentations are performed on the PolyU database to validate the proposed algorithm.*

**Keywords:** palmprint, biometrics, key points; midpoint; region of interest, ROI; principal lines; GLCM.

## I. INTRODUCTION

Biometric based recognition is the most popular human recognition by their biological features, inherent in each individual. Palmprint based biometric approach have been intensively developed over the past decade because they possess several advantages such as a rich set of features, high accuracy, high user friendly and low cost over other biometric systems. Palmprint recognition has five stages: palmprint acquisition, preprocessing, feature extraction, enrollment (database) and matching. The major approach for palmprint recognition is to extract feature vectors corresponding to individual palm image and to perform matching based on some distance metrics. Palmprint research employs high resolution or low resolution images. Principle

lines, wrinkles and texture-based features can be extracted from low resolution images. More discriminate features such as ridges, singular points and minutiae can be extracted using high resolution palm images. In our present work, we have used low resolution images to extract texture features.

Texture based feature extraction methods are widely adopted for palmprint identification because of their high performance. In the literature, numerous texture based approaches for palmprint recognition have been proposed. The palmprint textures can be obtained using techniques, such as Gabor wavelets[1], Fourier transformation[2], Cosine transformation [2,3], Wavelet transformation [4] and Standard Deviation [5].

In [6], fingerprint image is represented by co-occurrence matrices. Features are extracted based on certain characteristics of the co-occurrence matrix and then fingerprint classification is done using neural networks. A. Rampun et al.[7] proposed new texture based segmentation algorithm which uses a set of features extracted from Gray-Level Co-occurrence Matrices. Principal Component Analysis is used to reduce the dimensionality of the resulting feature space. Gaussian Mixture Modeling is used for the subsequent segmentation and false positive regions are removed using morphology.

Palmprint recognition based on haralick features was proposed by Ribaric et al.[9]. Haralick features are extracted from a sub-image and the matching process between the live template and the templates from the system database is performed in N matching modules. Fusion at the matching-score level is used and the final decision is made on the basis of the maximum of the total similarity measure. The experiments are performed on small databases (1324 hand images).The work

in [10] extracts haralick features along the principal lines and experiments were evaluated on small part of polyU database and shows poor performance (EER above 14%). An optimal thenar palmprint classification model is proposed by X. Zhu et al.[11]. Thirteen textural features of gray level co-occurrence matrix (GLCM) are extracted and support vector machine is used for classification. To the best of our knowledge, only few papers on palmprint identification using GLCM were reported in the literature. Most of them have used support vector machine and k-neural network classifiers and experiments have been performed on small databases and results reported in the literature were not promising. In the Literature, most of the feature extraction techniques are applied on fixed size ROI. ROI extraction is an important task for palmprint authentication. There are many schemes [8-10] were proposed to extract the ROI in palmprint images. Most of the researchers [11-16] have used fixed size ROI for palmprint. The fixed size ROI has limitations. The fixed size ROI covers smaller area and valued information is missing. The proposed algorithm focuses on extraction of Dynamic Region Of Interest (ROI) from the palmprint image. The performance of proposed ROI segmentation is verified using PolyU [17] database. This database consists of low-resolution images and is suitable for real-time application testing. The disadvantages of fixed size ROI affect the performance of recognition system. To overcome the disadvantages of fixed size ROI, the proposed algorithm extracts the texture features from dynamic ROI image. The rest of the paper is organized as follows. Details of dynamic ROI extraction [12] is described for completeness in Section 2. The texture feature extraction is described in Section 3. Section 4 described the proposed approach for palmprint identification. Experimental results are described in Section 5, followed by the conclusions in Section 6.

## 2. DYNAMIC ROI EXTRACTION

In developing ROI the method [12] is adopted. ROI extraction algorithm consists of two main stages. They are: Location of finger web points and Dynamic ROI extraction.

### 2.1 Location Of Finger Web Points

The following processes are performed to locate finger web locations using binary palmprint images

1. Convert the original gray scale Image into binary with grey value 0 or 1.
2. Boundary tracing algorithm is employed to find the palm border. Let  $S_t$  is the bottom-left point and considered as a starting point as shown in Fig 3. The tracing direction is along palm border in the counter clockwise direction until the starting point  $S_t$  is met again. The border pixels can be collected into a vector called Border Pixel Vector (BPV)
3. With  $S_t$  and BPV coordinates are known, we can calculate the Euclidean distance  $D_E$  between  $S_t$  and BPV using (1)

$$D_E(i) = (X_{S_t} - X_b(i) + (Y_{S_t} - Y_b(i))) \quad (1)$$

Where (  $X_{S_t}$  ,  $Y_{S_t}$  ) are the X and Y coordinates of the

$S_t$ , (  $X_b(i)$ ,  $Y_b(i)$  ) represents x and y coordinates of the  $i^{th}$  border pixel, and  $D_E(i)$  represents the Euclidian distance between  $S_t$  and  $i^{th}$  border pixel. A Distance distribution diagram shown in Fig 2 is constructed using the vector  $D_E$ . In the Fig 2., three local minima are the finger web points and are denoted by  $Fw1$ ,  $Fw2$  and  $Fw3$ .

4. The straight line  $L_s$  is formed by finger webs  $Fw1$  and  $Fw3$  as shown in Figure 3. Angle  $\theta$  between line  $L_s$  and the horizontal line is calculated using (2)

$$\theta = \tan^{-1} (Y_{Fw1} - Y_{Fw3} ) / (X_{Fw1} - X_{Fw3} ) \quad (2)$$

Where (  $X_{Fw1}$ ,  $Y_{Fw1}$  ) is the coordinate of  $Fw1$  and (  $X_{Fw3}$ ,  $Y_{Fw3}$  ) is the coordinate of  $Fw3$ .

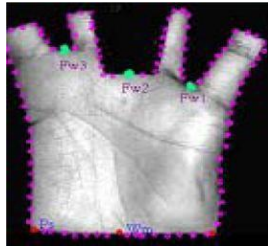


Fig. 1 Boundary pixels of palm image

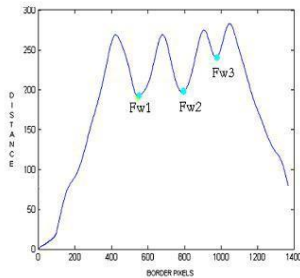


Fig. 2 Distance distribution diagram

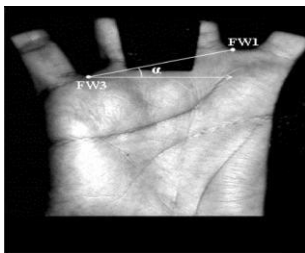


Fig. 3 Image Q after rotation with finger web point

## 2.2 DynamicROI Extraction

The steps for the ROI extraction from a palmprint image are given below.

1. To eliminate the influence of palm rotation and define the coordinate of ROI more conveniently, the palmprint image is rotated at an angle  $\theta$  (2) .
2. After rotation, the coordinates of finger web points changes. To get the new finger web points of the rotated image, we repeat step1 to 4 of section B. The new finger web points after rotation are denoted as FR1, FR2 and FR3.
3. In BVP array, first column represents X-coordinate and second column represents Y-coordinate values of border pixels. X-coordinate values and Y-coordinate values are stored in b1 and b2 matrix respectively

4. **For Width:** The maximum Y-coordinate value of b2- matrix is calculated using (3)

$$Y_m = \max(b_2) - k \quad (3)$$

Where  $k=15$  is chosen empirically for experimental

purpose. Then for this new  $Y_m$  there will be two X

coordinates (say  $X_1$  and  $X_2$ ) on the boundary as shown in Fig 4. and can be found from matrix. Now width of ROI is calculated using (4) and stored in  $W_d$

$$\text{Width } W_d = \text{abs}(X_1 - X_2) \quad (4)$$

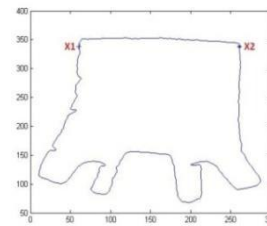


Fig. 4 Plotting  $X_1$  &  $X_2$  on boundary plot and inverted

5. **For Height:** To calculate the height we require maximum Y-coordinate ( $Y_{max}$ ) and minimum Y- coordinate ( $Y_{min}$ ). The  $Y_{max}$  can be calculated utilizing (5) by subtracting it from  $P$  which is the length of the image.

$$Y_{max} = P - Y_m \quad (5)$$

The  $Y_{min}$  can be calculated utilizing (6) by Finding the minimum Y-coordinate out of all three figure web points after complementing it with the length of image.

$$Y_{min} = \min(P - y_1, P - y_2, P - y_3) \quad (6)$$

where  $y_1, y_2$  and  $y_3$  are y-coordinate of figure web points FR1, FR2 and FR3 respectively. Height is the distinguishment between  $Y_{max}$  and  $Y_{min}$  and is calculated utilizing (7) shown in Fig 5 and stored in  $H_t$

$$\text{Height } H_t = \text{abs}(Y_{max} - Y_{min}) \quad (7)$$

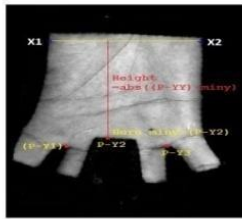


Fig. 5. For lowest left most point of rectangle

6. We have calculated height and width of palm print image. Now, to get maximum ROI Square region we require top leftmost point and lowest rightmost point, vividly it will be (X1, Ym) rightmost points and (X1, P-Ym) as the lowest leftmost point. The Dynamic ROI extracted is shown in Fig 6.

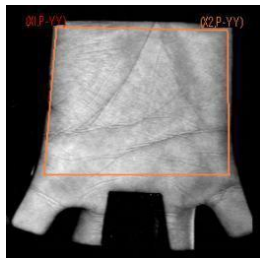


Fig.6 Palmprint Images and corresponding Dynamic ROI Extracted

### 3. TEXTURE FEATURE EXTRACTION USING GLCM

#### 3.1 Gray-Level Co-occurrence Matrix

Gray-Level Co-occurrence Matrix or GLCM [13,14] is a matrix that contains information about the distribution of intensities and information about the relative position of neighborhood pixels. As name suggests, it uses Grey-Scale images. Given a Grey-Scale Image I, the GLCM matrix P is defined as[13] :

$$P(i, \Delta x, \Delta y) = \sum_{j=1}^{M-\Delta x} \sum_{k=1}^{N-\Delta y} I(j, k) I(j+\Delta x, k+\Delta y) \quad (1)$$

Where  $W = 1/(M\Delta x)(N-\Delta y)$

$$\sum_{n=1}^{N-\Delta y} \sum_{m=1}^{M-\Delta x} A$$

$$A = \begin{cases} 1 & \text{if } f(m, n) = i \text{ and } f(m + \Delta x, n + \Delta y) = j \\ 0 & \text{elsewhere} \end{cases}$$

Where  $f(m, n)$  be the intensity at sample  $m$ , line  $n$  of the neighborhood,  $(i, j)$  is the index and  $(\Delta x, \Delta y)$  denotes the offset and the orientation respectively. Offset represents the distance between the interested neighborhood pixels and orientation represents the angle between interested neighborhood pixels. After calculation of GLCM we do the normalization by performing a divide operation on the product of  $M$  &  $N$ , where  $M$  &  $N$  are the dimensions of the Grey Scale image.

In our proposed methodology the local haralick features are calculated from normalized gray level co-occurrence matrices. Haralick introduced 14 statistical features [15] which are basically texture features which can be extracted from a GLCM matrix. The texture features [6-8] are Angular Second Moment, Contrast, Inverse Difference moment, Entropy, Correlation, Variance, Sum, Average, Sum Entropy, etc. In our investigation four features that can successfully characterize the statistical behavior (experimentally determined) are :

**Contrast** : The relative difference between light and dark areas of an image. Contrast is how dark to how light something is. The contrast makes the lighter colors more lighter, and the darker colors darker.

Contrast

$$= \sum_{n=0}^{G-1} \left\{ \sum_{i=1}^G \sum_{j=1}^G p(i, j) |i - j| = n \right\} \quad (2)$$

Where P is GLCM matrix and G is Grey Scale value

**Entropy**: It can be described as a measure of the amount of disorder in a system. In the case of an image, entropy is to consider the spread of states which a system can adopt. A low entropy system occupies a small number of such states, while a high entropy system occupies a large number of states. For example, in an 8-bit pixel there are 256 such states. If all such states are equally occupied, as they are in the case of an image, which has been perfectly histogram equalized, the spread of states is a maximum, as is the entropy of the image. On the other hand, if the image has

been threshold, so that only two states are occupied, the entropy is low. If all of the pixels have the same value, the entropy of the image is zero.

$$\text{Entropy} = \sum_{i=0}^{G-1} \sum_{j=0}^{G-1} p(i,j) \times \log(P(i,j))$$

Where P is GLCM matrix and G is Grey Scale value.

**Variance:** The variance is a measure of how far a set of numbers is spread out. It is one of several descriptors of a probability distribution, describing how far the numbers lie from the mean (expected value).

$$\text{Variance} = \sum_{i=0}^{G-1} \sum_{j=0}^{G-1} (i - \mu_x)^2 P(i,j) \quad (4)$$

Where P is GLCM matrix and G is Grey Scale value,  $\mu_x$  is the mean value.

**Correlation:** Measure that determines the degree to which two pixel values are associated.

$$\text{Correlation} = \frac{\sum_{i=0}^{G-1} \sum_{j=0}^{G-1} \{ i \times j \} P(i,j) - \{ \mu_x \times \mu_y \}}{\sigma_x \times \sigma_y} \quad (5)$$

Where P is GLCM matrix and G is Grey-Scale value,  $\mu_x, \mu_y$  are mean values &  $\sigma_x, \sigma_y$  are standard deviations along X and Y axis.

$$\mu_x = \sum_{i=0}^{G-1} i \sum_{j=0}^{G-1} P(i,j)$$

$$\mu_y = \sum_{i=0}^{G-1} i \sum_{j=0}^{G-1} jP(i,j)$$

$$\sigma_x^2 = \frac{\sum_{i=0}^{G-1} (i - \mu_x)^2 \sum_{j=0}^{G-1} P(i,j)}{\sum_{i=0}^{G-1} \sum_{j=0}^{G-1} P(i,j)}$$

$$\sigma_y^2 = \frac{\sum_{i=0}^{G-1} (j - \mu_y)^2 \sum_{j=0}^{G-1} P(i,j)}{\sum_{i=0}^{G-1} \sum_{j=0}^{G-1} P(i,j)}$$

GLCM matrices are calculated corresponding to different orientations ( 0, 45, 90, 135) with four different offset values. The above mentioned four haralick features are obtained from GLCM matrix created on sub-images of palmprint's ROI. By calculating this four texture features it is possible to see how they behave for different textures. The size of feature vector for a biometric template is M n – component feature vectors where M is the number of sub images defined by sliding window on the palmprint's ROI and n is the

number of local haralick features.

We have used the following parameters for our experiment: M×M=128×128 dimensions of palmprint ROI, g=256 number of grey levels, offset value  $\delta=1,2,3 \& 4, d \times d= 8 \times 8$  dimension of sliding window, t=4 sliding window translation step and  $\theta= 0,45,90$  and 135 degrees.

## 4. COMPUTATION OF FEATURE VECTOR AND MATCHING

### 4.1 Haralick Features Extraction

For the computation of the GLCM not only the displacement (offset value  $\delta$ ), but also the orientation between neighbor pixels must be established. The orientations can be horizontal (0°), Vertical (90), Right Diagonal(45) and Left Diagonal(135) degree respectively. GLCM matrices for each palmprint's ROI are calculated corresponding to different orientation( 0, 45, 90, 135 ) with four offset values. The local haralick features contrast, entropy, variance and correlation are obtained from normalized gray level co-occurrence matrices.

After the calculation of GLCMs, each GLCM is divided into 32x32 sub-matrices. For each such sub-matrix haralick features are calculated. There will be 64 such sub-matrices for each such GLCM. There are 4 GLCMs for each image. So total 256 such sub-matrices will be there for each image. So the size of feature vector for each image is: 4(offset values)× 4(four haralick features)×256(subimages). Therefore palmprint ROI is represented by 4096 features.

### 4.2 Matching

In matching process, the comparison is performed between template and query. In this paper, Euclidean distance similarity method is used to calculate the matching score. The Matching Score[16] between the template and query given by

$$\text{Matching Score} = 1 - \frac{\|x - y\|_2}{\|x\|_2 + \|y\|_2}$$

Where X is the feature vector of template and Y is the feature vector of query palmprint

calculated using haralick formulas. Norm is the Euclidean Norm which is the square root of the summation of square of the values i.e. If Vector P is [x y z] then Euclidean Norm [16] is:

$$||Norm|| = \sqrt{x^2 + y^2 + z^2}$$

The range of matching score is between 0 and 1. If the matching score is greater than a reference threshold, the user is considered as genuine otherwise imposter

### 5. EXPERIMENTAL RESULTS

The investigations were performed utilizing PolyU Palmprint database [17]. PolyU database comprises of 7,752 grayscale palm prints from 193 clients comparing to 386 separate palms. The experiment has been performed on a system of 2.0GHz CPU and 256 MB of RAM. The proposed algorithm is coded in MATLAB7 and executed on windows 2007 platform.

Most of the researchers [14-16] utilized the PolyU Palmprint database[14] and they extracted fixed size 128\* 128 ROI. Some of the researchers used the CASIA palmprint database [18] and extracted ROI sizes are 135\*135 & 128\*128. The developers at the IIT Delhi Touch less Palmprint Database [19] have extracted the ROI of size 150 x150. The result of the proposed algorithm is compared with fixed size ROI extraction algorithm[14] and stored in dynamic ROI database. The experiment demonstrates that fixed size ROI cover smaller area and valued information is missing where as dynamic size ROI extracts maximum size ROI and 99.9% ROIs without background information. The ROI images we obtained from each palm image had maximum Size of ROI 201\*174 and minimum Size of ROI 137\*163.

The proposed GLCM based texture feature extraction algorithm is applied on both static and dynamic ROI PolyU Palmprint database and feature vector for each image in the database is computed and stored in the respective databases. The performance evaluation of proposed system is evaluated using three measures: : 1. False Acceptance Rate (FAR), 2. False Rejection Rate (FRR) and 3 .Equal Error Rate (EER).

The False-Rejection-Rate (FRR) indicates the frequency of rejected users who are not imposters. It is one of the most important metrics in a biometric system, since the restriction of access to genuine users is a considerable flaw. It is calculated as:

$$FRR = \frac{\text{Total number of actual clients falsely reject}}{\text{Total number of comparisons}} \times 100$$

Another important metric is the *False-Acceptance-Rate (FAR)*, which expresses the portion of false identity claims that are incorrectly accepted, by so depicting the frequency of fraudulent accesses. It is defined as:

$$FAR = \frac{\text{Total number of imposters falsely accep}}{\text{Total number of comparisons}} \times 100$$

Finally, the Equal-Error-Rate (EER) is defined as the rate at which the FAR is equal to the FRR. A very low number for ERR indicates a system with a good balance of sensitivity but is not necessarily the adequate operating point. Specific system requirements could have constraints for a low FAR or FRR value. Table 1. gives the experimented results of FAR and FRR rates of texture features extraction using GLCM from Static ROI and Dynamic ROI. The plot between FAR and FRR at various thresholds for static ROI and Dymamic ROI is shown in Fig. 7 and Fig 8 respectively.

EER values of texture feature extraction through static ROI are 0.23 and through dynamic ROI is 0.03. The Identification rate of proposed dynamic ROI approach is better compared to static ROI. Table 2 presents the performance comparison of our proposed approach with existing approaches.

**Table 1.** FAR and FRR rates of Texture features extraction using GLCM from Static ROI and Dynamic ROI

Thres hold	Texture Features(GLC M) from Static ROI		Texture Features(GLCM ) from Dynamic ROI	
	FRR	FAR	FRR	FAR
0.58	0.8873	0.02	0.15	0

0.6	0.867 3	0.02	0.12	0.01
0.62	0.857	0.03	0.09	0.03
0.7	0.706 6	0.04	0.05	0.03
0.72	0.658 3	0.04	0.03	0.03
0.8	0.391 7	0.08	0.006	0.05
0.84	0.239 7	0.23	0.004	0.06
0.88	0.097	0.4	0.000 6	0.12
0.9	0.047	0.5	0.000 3	0.14

**Table 2.** Performance comparison of proposed approach with existing approaches.

S.No	Author and Ref No.	Database size	EER	
			Static ROI	Dynamic ROI
1.	Mansoor et al[20]	7,752	0.1562	---
2.	Wu et al[21]	3,200	2.11	---
3.	Badrinath et al[22]	3,855	0.002	---
4.	Hemanth et al[23]	7,752	0.17	0.25
5.	Proposed approach	7,752	0.23	0.03

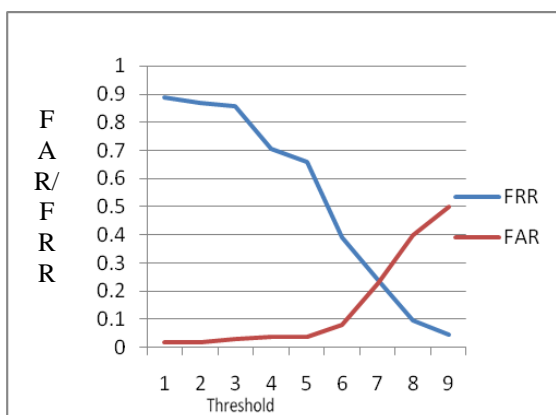


**Fig 7.** FAR and FRR at various thresholds for Static ROI

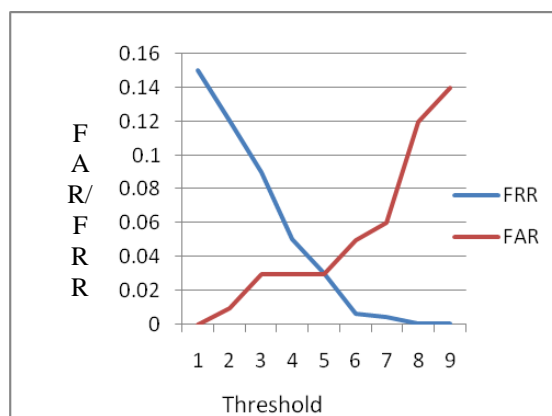


**Fig 8.** FAR and FRR at various thresholds for Dynamic ROI

**6. CONCLUSION**

In this paper, an efficient palmprint identification approach based on texture feature using GLCM through dynamic ROI is proposed. The experimental results show that GLCM through dynamic ROI is better when compared to static ROI approach. From the experimental results of identification, it can be concluded that, the proposed approach yields better results in terms of EER compared with existing approaches.

**REFERENCES**

1. Wang Xuan, Lei Li and Wang Mingzhe, (2012), "Palmprint Verification based on 2D Gabor Wavelet and Pulse Coupled Neural Network", *Knowledge-Based Systems*, Elsevier Science Publishers, Vol 27, pp. 451-455.
2. H Imatiaz and S A Fattah, (2011), "A Spectral Domain Dominant Feature Extraction Algorithm for Palmprint Recognition", *International Journal of Image processing (IJIP)*, Vol 5, pp. 130-144,
3. Manisha , Madhuri and Neena, (2009), "Texture Based Palmprint Identification Using DCT features", *International conference on*

- Advances in Pattern Recognition*, Vol 42, pp. 221-224.
4. Pritee Khanna, Deepti Tamrakar,(2010), “Analysis of palmprint Verification using Wavelet filter and competitive code”, *International conference on computational Intelligence and communication Network*, pp. 20-25.
  5. Rafael C, Gonzalez, Richard E woods, (2009),”Digital Image Processing”, *Pearson Education*.
  6. M. Yazdi, K. Gheysari, (2008),“A New Approach for the Fingerprint Classification Based on Gray-Level Co-Occurrence Matrix“, *International Journal of Computer and Information Science and Engineering* ,pp.171-174.
  7. Andrik Rampun, Harry Strange, Reyer Zwiggelaar, (2013),“Texture segmentation using different orientations of GLCM features”, *6th International Conference on Computer Vision / Computer Graphics Collaboration Techniques and Applications, MIRAGE ’*, pp. 519-528.
  8. Ying Chen, Fengyu Yang, Huiling Chen, (2013),” An Effective Iris Recognition System Based on Combined Feature Extraction and Enhanced Support Vector Machine Classifier” , *Journal of Information & Computational Science*, pp . 5505–5519.
  9. S. Ribaric, M. Lopar. (2012),“Palmprint recognition based on local Haralick features”, *in: Proc. IEEE Melecon*, Vol. 18, pp. 657- 660.
  10. D. S. Martins, (2013),“Biometric recognition based on the texture along palmprint principal lines”, *Faculdade de Engenharia da Universidade do Porto*.
  11. X. Zhu, D. Liu, Q. Zhang.(2011), “Research of Thenar Palmprint Classification Based on GLCM and SVM”, *Journal of Computers*, Vol. 6, pp. 1535-1541.
  12. Y.L Malathi latha, M.V.N. K Prasad, Proc. of Int. Conf. on Advances in Computer Science, AETACS,Elsevier,2013.
  13. Albrechtsen, Fritz. "Statistical texture measures computed from gray level co-ocurrence matrices." *Image Processing Laboratory, Department of Informatics, University of Oslo* ,pp 1-14,2008.
  14. Eleyan, Alaa, and Hasan Demirel. "Co-occurrence based statistical approach for face recognition." *Computer and Information Sciences*, Vol, 3,pp.611-615,IEEE, 2009.
  15. Wang, Song, and Jiankun Hu. "Alignment-free cancelable fingerprint template design: A densely infinite-to-one mapping (DITOM) approach." *Pattern Recognition*, pp. 4129-4137, 2012.
  16. Wang, Song, and Jiankun Hu. "Alignment-free cancelable fingerprint template design: A densely infinite-to-one mapping (DITOM) approach." *Pattern Recognition*, pp. 4129-4137, 2012.
  17. <http://www4.comp.polyu.edu.hk/~biometrics/> Poly palmprint database available
  18. CASIA Palmprint Database, <http://www.cbsr.ia.ac.cn/PalmDatabase.html>
  19. 23 IIT Delhi Touchless Palmprint Database version1.0, [http://web.iitd.ac.in/~ajaykr/Database\\_Palm.html](http://web.iitd.ac.in/~ajaykr/Database_Palm.html)
  20. Mansoor, A.B., Masood, H., Mumtaz, M. and Khan, S.A. ‘A feature level multimodal approach for palmprint



- identification using directional subband energies', *Journal of Network and Computer Applications*, Vol. 34, No. 1, pp.159–171, 2011.
21. X.Q. Wu, K.Q. Wang and D. Zhang,, "Wavelet Energy Feature Extraction and Matching for Palmprint Recognition", *Journal of Computer Science & Technology*, Vol. 20, No. 3, pp. 411–418,2011.
  22. Badrinath, G.S. and Gupta, P. 'Stockwell transform based palmprint recognition', *Applied Soft Computing*, Vol. 11, No. 7, pp.4267–4281, 2011.
  23. Henatha kumar kulluri, M.V. N. K Prasad, Aruna Agarwal,"Palmprint identification and verification based on wide principal lines through dynamic ROI", *International Journal of biometrics*, Vol 7, No. 1, 2015.